J Mol Model (2011) 17:1173–1182
DOI 10.1007/s00894-010-0821-6

ORIGINAL PAPER

Structure-based *in-silico* rational design of a selective peptide inhibitor for thymidine monophosphate kinase of *mycobacterium tuberculosis*

Manoj Kumar · Sujata Sharma · Alagiri Srinivasan · Tej P. Singh · Punit Kaur

Received: 25 March 2010 / Accepted: 22 July 2010 / Published online: 11 August 2010

Abstract Tuberculosis still remains one of the most deadly infectious diseases. The emergence of drug resistant strains has fuelled the quest for novel drugs and drug targets for its successful treatment. Thymidine monophosphate kinase (TMPK) lies at the point where the salvage and *de novo* synthetic pathways meet in nucleotide synthesis. TMPK in *M.tb* has emerged as an attractive drug target since blocking it will affect both the pathways involved in the thymidine triphosphate synthesis. Moreover, the unique differences at the active site of TMPK enzyme in *M.tb* and humans can be exploited for the development of ideal drug candidates. Based on a detailed evaluation of known inhibitors and available three-dimensional structures of TMPK, several peptidic inhibitors were designed. *In silico* docking and selectivity analysis of these inhibitors with TMPK from *M. tb* and human was carried out to examine their differential binding at the active site. The designed tripeptide, Trp-Pro-Asp, was found to be most selective for *M.tb*. The ADMET analysis of this peptide indicated that it is likely to be a drug candidate. The tripeptide so designed is a suitable lead molecule for the development of novel TMPK inhibitors as anti-tubercular drugs.

Keywords Drug design · Molecular docking · *M.tb* · Peptide inhibitor · Thymidine monophosphate kinase

M. Kumar · S. Sharma · A. Srinivasan · T. P. Singh · P. Kaur (✉)
Department of Biophysics, All India Institute of Medical Sciences, Ansari Nagar,
New Delhi 110 029, India
e-mail: punitkaur1@hotmail.com

Introduction

Mycobacterium tuberculosis (*M.tb*) is the main causative agent for tuberculosis (TB) in humans. It is the most prevalent infectious disease and remains the leading cause of fatalities amongst them [1]. Chemotherapy with four front-line drugs (rifampicin, isoniazid, pyrazinamide and ethambutol) for at least six months, due to the absence of an effective vaccine, still remains the existing treatment regimen [2]. The deadly synergy of *M.tb* with HIV coupled with increasing drug resistance has become the latest public health concern around the world [3]. This scenario has made it imperative to identify new drug targets and develop novel anti-TB drugs that shorten the long duration for effective drug therapy [4, 5]. Thymidine monophosphate kinase of *M.tb* (TMPK*mt*) is one such recent potential target which has gained immense significance for the development of anti-TB drugs.

TMPK (EC 2.7.4.9) is the last specific enzyme in the pyrimidine biosynthetic pathway and catalyses the ATP-dependent reversible phosphorylation of deoxythymidine 5′monophosphate (dTMP) into deoxythymidine 5′diphosphate (dTDP) [6]. It is situated at the junction of *de novo* pathway (deoxyuridine monophosphate into dTMP by Thymidylate synthase) and salvage pathway (deoxythymidine into dTMP by Thymidine kinase) for the synthesis of deoxythymidine 5′triphosphate (dTTP) which is essential for DNA replication. Thus, TMPK*mt* is crucial for cell proliferation as well as survival of the organism [7].

The nucleoside analogues 3′-deoxythymidine (dT) and 3′-azedo-deoxythymidine (AZT) are direct inhibitors of TMPK*mt* with moderate inhibition (K_i value of 27 μM and 28 μM respectively) having seven-fold and 16-fold selectivity over human TMPK (TMPK*h*), respectively [8, 9].

Several pyrimidine and purine nucleotide analogues have also been developed and their inhibitory activities studied [10–18]. A major challenge in anti-tubercular drug design is the low permeability of the mycobacterial cell wall for phosphorylated nucleosides which are at the same time highly prone to degradation by serum phosphatases. Moreover, the N-glycosidic linkage between ribose sugar and thymine base is susceptible to cleavage by human thymidine phosphorylase [19]. Several novel compounds have been identified using structure-based design approach by replacing sugar moiety of nucleoside analogues with benzyl group, naphthalimide, naphtholactam or naphthosultam [20, 21]. The rational approach based on virtual screening method with Maybridge compounds database has identified three novel compounds with minimal inhibitory concentration (MIC) of 3.12 μM [22]. The best reported inhibitor so far has potency in lower micro-molar range and most of the identified inhibitors for TMPK*mt* do not possess good selectivity index (SI). Therefore, there exists an urgent need for the inhibitor with high affinity and selectivity for TMPK*mt*.

TMPK*mt* and TMPK*h* belong to the Nucleoside monophosphate kinase (NMPK) family and despite their low sequence identity both have similar structural features which comprises the Rossman fold. Their enzymatic action depends on the conformations adopted, open, partially closed or closed, by them. The variation in the conformation of the protein is due to movement of P-loop and LID region based on the presence or absence of substrates. The deviation in the P-loop and LID region is limited in TMPK*mt* whereas in TMPK*h* it can adopt open, partially closed or closed conformations. TMPK*mt* is found in closed conformation in the presence of dTMP and absence of ATP (a SO_4^{2-} or acetate ion occupies the β–phosphate position of ATP) [23–25] while in TMPK*h*, it has a partially closed conformation even in the presence of dTMP and ATP [26–28]. The TMPK*mt* unlike TMPK*h* requires the transient binding of a magnesium ion for the phosphate transfer to take place [23–28]. The magnesium ion is required for the proper positioning of catalytic residues through polar interactions with the key residues in the P-loop (Asp9) and LID region (Asp163) leading to closed conformation of TMPK*mt*. The 3′azidodeoxythymidine monophosphate (AZTMP) inhibits TMPK*mt* as its azido group replaces the magnesium ion while it is a substrate for TMPK*h* [25, 27]. Though their binding sites are highly conserved, there are few crucial differences among the binding sites residues in the TMPK*mt* and TMPK*h*. The residues in TMPK*mt* binding site are Arg14, Tyr39 and Asn100 while the corresponding residues in TMPK*h* are Ser20, Arg45 and Gly102, respectively. Hence, these structural and functional differences can be exploited to design selective inhibitors for TMPK*mt*.

In an effort to identify more potent and selective inhibitors of TMPK*mt*, we have undertaken a study of small peptide inhibitors as potential lead compounds. Based on the crystal structures of TMPK*mt* complexed with AZTMP (PDB Id: 1W2H) [25] and TMPK*h* complexed with AZTMP (PDB Id: 1E99) [27], the rational structure-based approach has been employed for designing a set of small peptides. Docking and scoring of these peptides using Discovery Studio (DS) 1.7 have led to the identification of more potent as well as more selective inhibitors for TMPK*mt* as compared to the inhibitors proposed so far.

Materials and methods

The starting point for the computational studies was the X-ray crystal structure of TMPK*mt* complexed with AZTMP [PDB Id: 1W2H] [25]. All computations were carried out using the software DS 1.7 [29].

Receptor setup

The target protein TMPK*mt* [PDB Id: 1W2H] and TMPK*h* [PDB Id: 1E99] from the Protein Data Bank (PDB) was taken without the crystallographic water molecules [30], the ligand AZTMP was extracted and hydrogens added. The positions of the hydrogen atoms was optimized using the all atom CHARMm (version-c32b1) forcefield [31, 32] and the adopted basis set Newton Raphson (ABNR) method with distance-dependent dielectric model until the root mean square (r.m.s) gradient was less than 0.05 kcal mol^{-1} $Å^{-1}$. The minimized protein was defined as the receptor using the binding site module. The volume of the ligand method modified to accommodate all the important interacting residues in the active site of TMPK*mt* was used to define the binding site. The input site sphere was defined over the site, with a radius of 5 Å from the centre of binding site. The protein, thus characterized, was taken as the target receptor for the docking procedure.

Ligand setup

Using the build-and-edit module of DS 1.7, the peptide of the desired sequence with a protonated amino group and a deprotonated carboxyl group was built; all atom CHARMm forcefield parameterization was assigned and then minimized using the ABNR method. A conformational search of the peptide was carried out using a simulated annealing molecular dynamics approach. The ligand was heated to a temperature of 700 K and then annealed to 200 K. Each simulation lasted for 5 ps. Thirty cycles were carried out sequentially using the output of the previous cycle. The conformation obtained at the end of each cycle was further

subjected to local energy minimization by employing ABNR method. The 30 energy minimized structures were then superimposed and the lowest energy conformer in the major cluster was taken to be the most probable conformation.

Docking and scoring

The LigandFit [33] docking protocol was used to dock the ligands with TMPK*mt* and TMPK*h*. The LigandFit docking algorithm combines a shape comparison filter with a Monte Carlo conformational search to generate docked poses consistent with the binding site shape. These initial poses are refined by rigid body minimization of the ligand with respect to the grid-based calculated interaction energy using the Dreiding forcefield [34]. The receptor protein was kept fixed during docking. The docked poses were further minimized using all-atom CHARMm (version c32b1) forcefield and smart minimization method (steepest descent followed by conjugate gradient) until the r.m.s gradient for potential energy was less than 0.05 kcal mol^{-1} $Å^{-1}$. The atoms of ligand and the side chains of the residues of the receptor within 5 Å from the center of the binding site were kept flexible during minimization.

The final step in docking is the scoring of the refined docked poses. This was done using the "score ligand poses" protocol wherein the LUDI III score [35–37] was used to score the refined poses. The ligand pose which corresponded to the highest LUDI III score was taken as the best docked pose [38].

ADMET analysis

The advent of predictive tools for screening of absorption, distribution, metabolism, excretion and toxicity properties (ADMET) of drugs has revolutionized the drug discovery process. This technology enables filtering of weak drug candidates. This elimination in early drug discovery process helps to decrease the number of drug failures in the clinical trials. Traditionally these predictive tools were applied at the end of the drug discovery process, but are now utilized during the initial phase of drug development. The removal of molecules with poor pharmacokinetic properties in the early stage leads to significant cost savings. The ADMET descriptor and TOPKAT protocol available in DS 1.7 were used to predict these properties. The Lipinski's rule of 5 was also used to determine the biological activity or drug-likeness of the designed inhibitor [39, 40].

Molecular dynamics

In order to check whether the designed inhibitor remains bound in the presence of explicit solvent, a molecular dynamics (MD) simulation was carried out on a fully hydrated model using explicit spherical boundary with harmonic restraint.

The final receptor-ligand complex was first solvated using the explicit solvent model. The standard dynamics cascade protocol [41] available in DS 1.7 was used with a time step of 1 fs. The energy minimization of the hydrated model was the first step in the MD simulation. The backbone of the refined receptor was kept fixed. The minimized hydrated complex was then subjected to a MD simulation in three stages. In the first stage the temperature of the system was raised from 50 to 300 K over 2 ps. Next the system was equilibrated for 20 ps, and finally the production run was carried out for another 150 ps.

Results and discussion

Validation of the docking methodology

The docking protocol was first validated with already known structures available in the PDB (PDB Id: 1W2H and 1G3U) [23, 25]. A deviation observed in the conformation of the docked ligand on superimposition with that from the crystal structure is used to verify the docking protocol. The correlation between the predicted and experimental binding affinity (K_i) and position of the docked ligand produced by the program to that observed in the crystal structure validates the experimental and theoretical data. A successful scoring function is the one in which the root mean square (r.m.s.) deviation of the best docked pose is less than 2 Å from the experimental one. Hence, both the known inhibitor AZTMP and natural substrate dTMP were docked in the dTMP binding site of TMPK*mt* after extracting the ligand from the crystal structure. The docked pose having the highest LUDI III score gave the least r.m.s. deviation with respect to the crystal conformation for both the ligands. The LUDI III is an empirical scoring function which is used to predict the binding affinity of the ligands when complexed with the protein. It is based on the free energy of binding (LUDI III score$=-100$ $\log K_i$ and $\log K_i = -\Delta G / 2.303\ RT$) and has a standard error of 1.75 kcal mol^{-1}. The corresponding error in the estimated binding affinity using LUDI III scoring function can vary up to 20 times the experimental value of binding affinity [37].

The orientation and position of dTMP (Fig. 1a) and AZTMP (Fig. 1b) in both crystal structure and docked structure are seen to overlap with a positional r.m.s. deviation of 1.6 Å and 1.3 Å respectively. The predicted binding affinity (K_i) of AZTMP for TMPK*mt* using LUDI III scoring function was found to be 8.13 μM which is in good agreement with the observed K_i value of 10 μM [42]. In the case of dTMP, the binding affinity was found to be

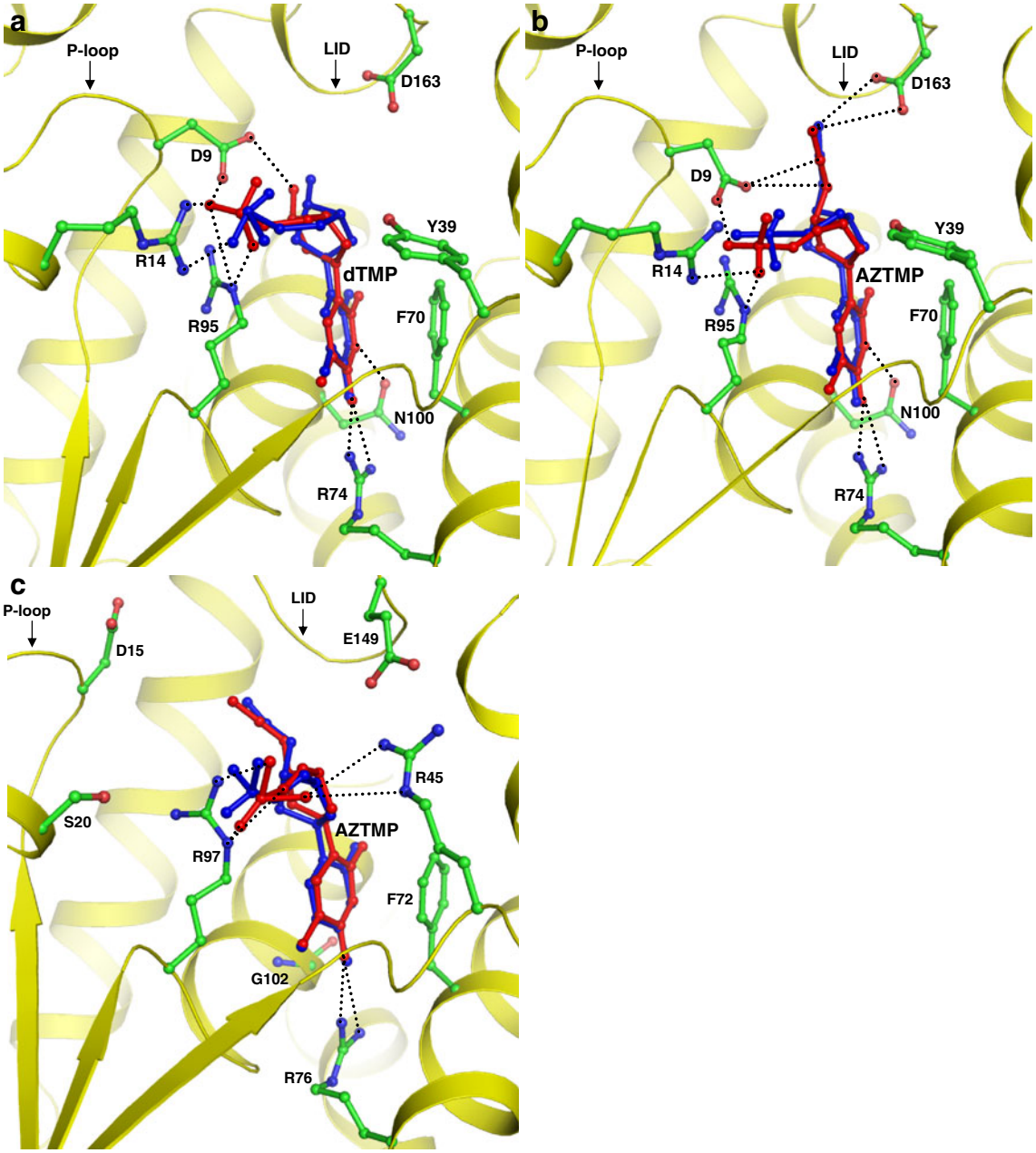

Fig. 1 Docked position of (**a**) dTMP in TMPK*mt*, (**b**) AZTMP in TMPK*mt* and (**c**) AZTMP in TMPK*h* (red, ball-and-stick) superimposed on the crystal structure position (blue, ball-and-stick) in respective TMPK (yellow, cartoon) showing the selected active site residues (ball and stick and colored by atom type). Hydrogen bonds are shown as black, dotted lines. All figures were produced using PyMol v0.99 [45]

1.3 μM which agrees with the experimental K_m value of 4.5 μM [12].

The validation of the docking methodology was also carried out for the inhibitor AZTMP with TMPK*h*. The superposition of the docked AZTMP and that observed in the crystal structure gave an r.m.s. deviation of 1.2 Å indicating a good overlap of these two positions (Fig. 1c). The predicted K_i value of 24 μM agrees with the observed value of 12 μM [28]. Thus, these results validated the docking and scoring methodology used.

Design of a peptide inhibitor and docking of the designed inhibitor with TMPKmt

Most of the reported inhibitors of TMPK*mt* contain an aromatic ring (Fig. 2a). Moreover, it has also been consistently observed in the available crystal structures of

Fig. 2 **a**) Chemical structure of dTMP, substrate of TMPK and known inhibitor AZTMP of TMPK*mt* **b**) Chemical structure of the designed peptides for TMPK*mt* ▶

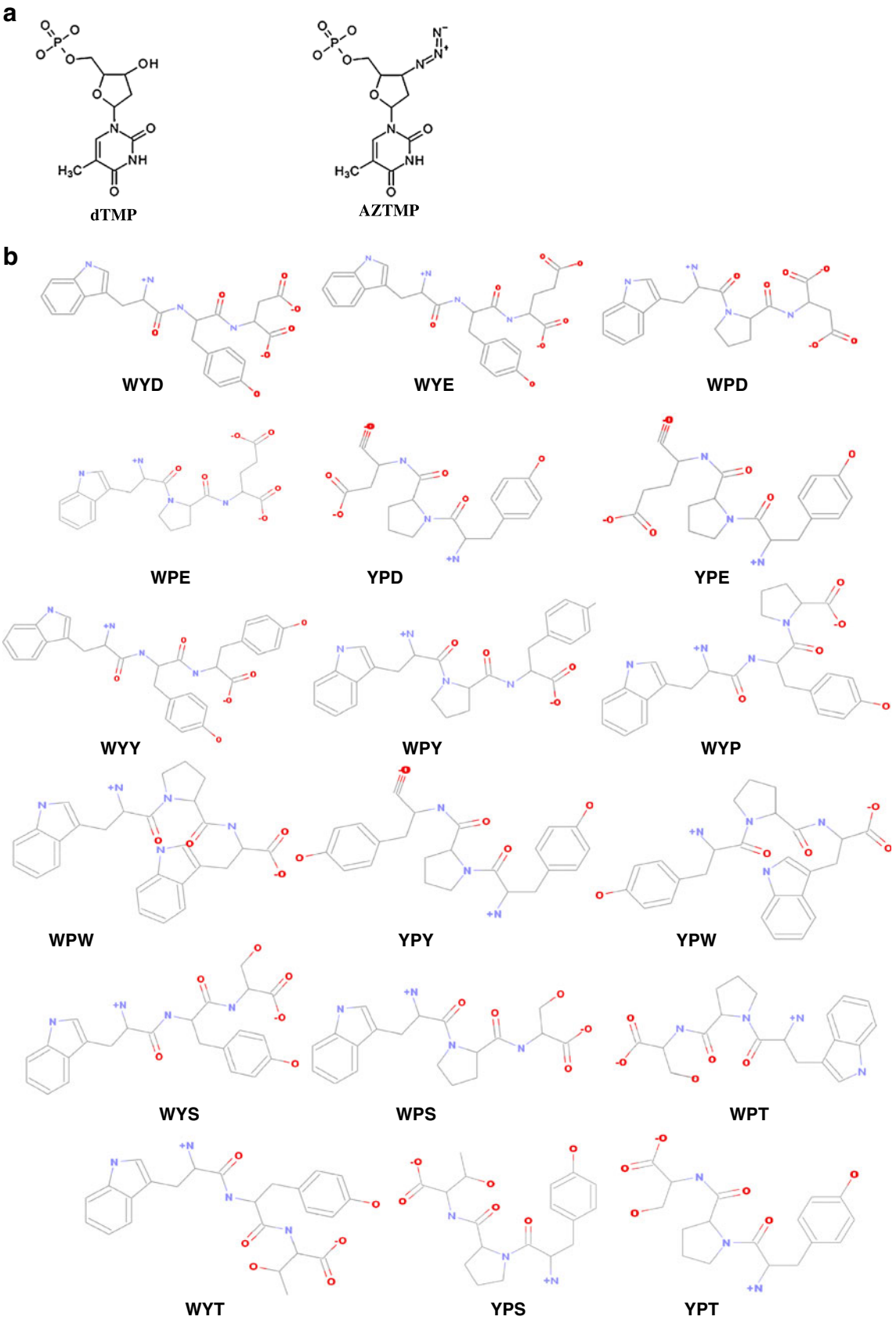
a
dTMP
AZTMP
b
WYD
WYE
WPD
WPE
YPD
YPE
WYY
WPY
WYP
WPW
YPY
YPW
WYS
WPS
WPT
WYT
YPS
YPT

Table 1 Peptide sequences and their predicted activity

Predicted K_d value (μM) for binding with		
Peptide sequence	TMPK*mt*	TMPK*h*
WYD	0.0063	0.21
WYE	0.00014	0.12
WPD	**0.000018**	**0.43**
WPE	0.0078	0.0037
YPD	0.046	0.58
YPE	0.02	6.2
WYY	0.00051	0.060
WPY	0.0068	0.17
WYP	0.00019	0.12
WPW	0.00091	0.024
YPY	0.0040	0.21
YPW	0.028	0.00047
WYS	0.054	1.7
WPS	0.0025	0.025
WPT	0.0047	0.014
WYT	0.000087	0.0081
YPS	0.15	0.72
YPT	0.076	1.0

TMPK*mt* complexed with inhibitors that the aromatic ring of the inhibitor has stacking interactions with Phe70 (a highly conserved residues among TMPKs). The substitution of thymidine analogue with 5' thiourea substituted sugar increases the affinity and selectivity for TMPK*mt* over other classical analogues [15]. Recently, inhibitors having higher affinity for TMPK*mt* have been developed by replacement of sugar moiety with naphthyl moiety and introducing a spacer with *cis* double bond in thymidine using rational design approach [21]. Modeling studies predicted that the higher affinity was due to increased aromatic interactions of *cis* double bond of spacer with Tyr103 and Tyr165, edge-to-face stacking interactions of naphthosultam ring with Tyr39 and the presence of an additional hydrogen bond with guanidium group of Arg95 [21]. Thus, several tripeptide sequences containing at least one aromatic amino acid residue were designed. Each of the tripeptide was docked after a conformational search as described in methods. A list of the sequences of designed peptide along with their corresponding predicted activities and their chemical structure are given in Table 1 and Fig. 2b respectively. The highest affinity with K_i value of 18.2 picomolar (pM) was observed with the tripeptide sequence $NH3^+$-Trp-Pro-Asp-COO^- (WPD).

The final docked position of the designed inhibitor is shown in Fig. 3, and the list of contacting residues (up to 4 Å) is given in Table 2. The tripeptide {represented by (P)} occupies a position in the binding site pocket of the protein similar to AZTMP (Fig. 3a). Additionally it extends into the ATP binding pocket occupying it partially. Thus, the designed tripeptide covers a larger area of the binding pocket. A number of hydrogen bonds were observed between WPD and TMPK*mt*. The N-terminal of the designed inhibitor (WPD) forms hydrogen bonds with side chain of residues Asp163 and Glu166 of LID region. The carboxy-terminal forms a network of hydrogen bonds with the backbone nitrogen atoms of P-loop residues (Gly10, Ala11, Gly12) and side chain nitrogen of Lys13 (Fig. 3b). The OD1 and OD2 of Asp (P) form hydrogen bonds with Arg14 guanidium moiety. The backbone oxygen of Pro (P) also forms hydrogen bonds with side chain atoms of Asp9 and Arg95 similar to that observed in dTMP and AZTMP. The aromatic ring of Trp (P) has face-to-face π-π interactions with conserved residue Phe70. In addition, it has edge-to-face aromatic interactions with side chain of

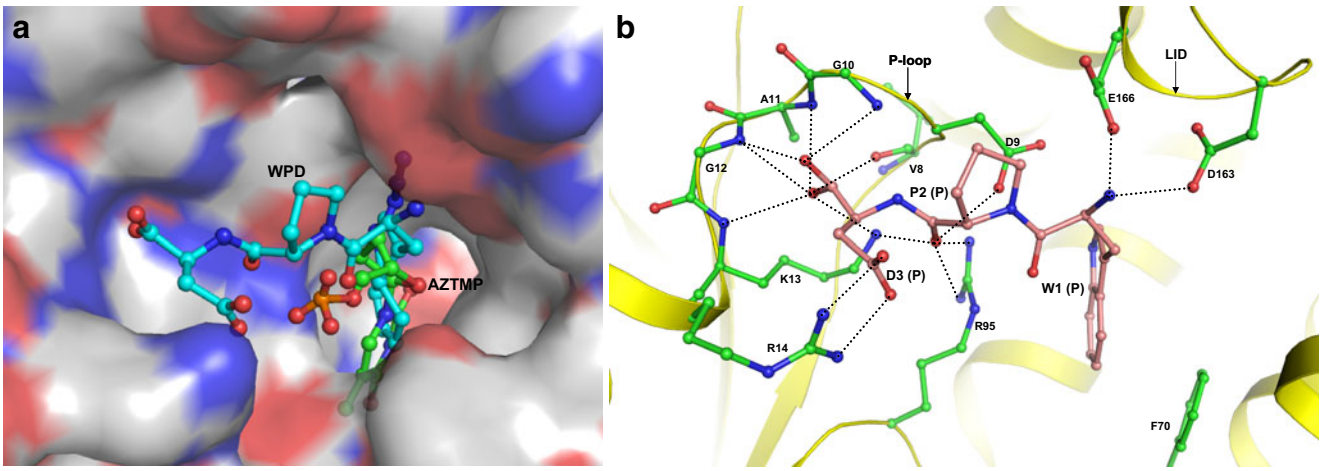

Fig. 3 **a**) Final docked position of the designed peptide inhibitor, WPD (blue, ball-and-stick) superimposed on AZTMP (magenta, ball-and-stick) complexed with TMPK*mt*. The coloring and rendering are similar to Fig. 1 **b**) Final docked complex of TMPK*mt* with the designed inhibitor, WPD (ball-and-stick, colored by atom type)

Table 2 Docking of various known ligands with TMPK*mt* and TMPK*h*

Ligand	Docked with	Docked energy (kcalmol^{-1})			Contacting residues (up to 4.0Å) in final docked position (hydrogen bonded residues are highlighted in bold)
		Steric	Electrostatic	Total	
dTMP	TMPK*mt*	−29.06	−126.78	−155.84	**D9**, K13, **R14**, F36, P37, F70, **R74**, **R95**, S99, **N100**, Y103, Y165
AZTMP	TMPK*mt*	−37.48	−80.18	−117.66	**D9**, K13, **R14**, F36, P37, Y39, F70, **R74**, D94, **R95**, Y96, S99, **N100**, **D163**, Y165, E166
WPD	TMPK*mt*	−28.97	−237.90	−266.87	**V8, D9**, **G10**, **A11**, **G12**, **K13**, **R14**, P37, F70, **R95**, Y103, **D163**, Y165, **E166**
AZTMP	TMPK*h*	−31.99	−86.63	−118.62	F42, P43, **R45**, L57, F72, **R76**, **R97**, Y98, S101, F105, E149, Y151, E152, Q157
WPD	TMPK*h*	−17.81	−149.46	−167.27	**S20**, R41, F42, P43, **R45**, L57, **R97**, F105, **E149**, Y151, **E152,** ADP

Tyr103. Hence, the designed inhibitor forms a greater number of interactions than the conserved interactions present in the dTMP and AZTMP with TMPK*mt*. These additional interactions are reflected in the lower docking energy (−266.87 kcal mol^{-1}) (Table 2).

Molecular dynamics simulation of a fully hydrated model of the final docked complex

The effect of solvent on the binding of the designed peptide inhibitor was studied by a MD simulation of a fully hydrated model. During the production phase of 150 ps following the initial heating and equilibration phases, the total energy and the simulation temperature were found to remain steady with little fluctuation. The snapshots of the dynamics trajectory at 0, 25, 50, 75, 100, 125 and 150 ps of the production run are shown in Fig. 4, while the corresponding interaction energies and interaction sets have been provided in Table 3. Table 4 gives the selectivity of designed ligand.

The results indicate that the ligand as a whole moves into a more stable position with a lower docked energy than the initial starting point in the presence of explicit solvent molecules (Table 3). There was no significant difference in the binding position and conformation of designed inhibitor, WPD, except for a slight change in the position of Pro (P) after molecular dynamics simulation. The N-terminal nitrogen of the ligand moves toward Asp163 and forms an additional hydrogen bond with OD1 keeping the initial hydrogen bond with OD2 of Asp163 and OD2 of Glu166 intact. This leads to additional non-polar interactions of Trp (P) with Leu52. Similarly, the backbone nitrogen of Pro (P) forms a hydrogen bond with OD1 of Asp9 which was not observed earlier. The hydrogen bond of carboxy-terminal oxygen with backbone nitrogen of Val8 was retained only after 100 ps of production phase while the remaining

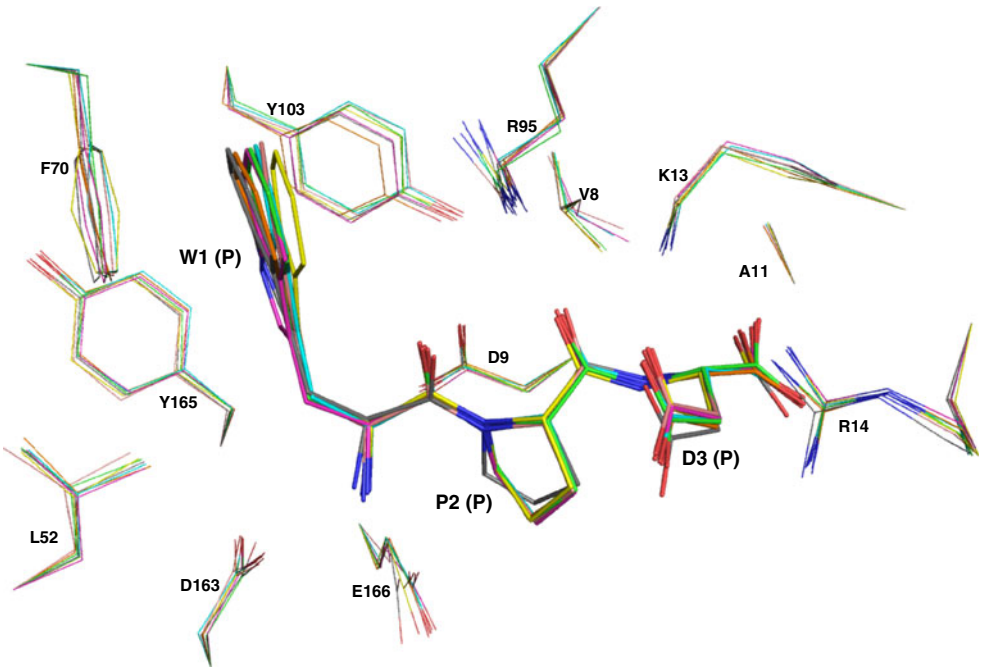

Fig. 4 Molecular dynamics trajectory for the docked complex. Snapshots of the designed peptide and the TMPK*mt* active site residue conformers extracted from the production dynamics trajectory at the time intervals of 0, 25, 50, 75, 100, 125, and 150 ps. The peptide is shown in thin stick and binding site residues are shown as lines

Table 3 Fully hydrated dynamics simulation results of docked complex TMPK*mt* - WPD

Docked energy of ligand (kcalmol^{-1}) With solvent and enzyme				With enzyme only			
Time (ps)	Steric	Electrostatic	Total	Steric	Electrostatic	Total	Contacting residues (up to 4.0Å) (hydrogen bonded residues are highlighted in bold)
0	−27.87	−528.28	−556.15	−35.06	−726.68	−761.74	V8, **D9**, **G10**, **A11**, **G12**, **K13**, **R14**, L52, F70, **R95**, Y103, **D163**, Y165, **E166**
25	−27.19	−553.67	−580.86	−30.13	−782.68	−812.81	V8, **D9**, **G10**, **A11**, **G12**, **K13**, **R14**, L52, F70, **R95**, Y103, **D163**, Y165, **E166**
50	−24.99	−566.92	−591.91	−31.45	−811.62	−843.07	V8, **D9**, **G10**, **A11**, **G12**, **K13**, **R14**, L52, F70, **R95**, Y103, **D163**, Y165, **E166**
75	−23.84	−540.78	−564.62	−25.13	−771.94	−797.07	V8, **D9**, **G10**, **A11**, **G12**, **K13**, **R14**, L52, F70, D94, **R95**, Y103, **D163**, Y165, **E166**
100	−24.17	−556.42	−580.59	−28.75	−814.17	−842.92	V8, **D9**, **G10**, **A11**, **G12**, **K13**, **R14**, L52, F70, **R95**, Y103, **D163**, Y165, **E166**
125	−23.88	−550.02	−573.90	−27.23	−782.28	−809.51	**V8**, **D9**, **G10**, **A11**, **G12**, **K13**, **R14**, L52, F70, D94, **R95**, Y103, **D163**, Y165, **E166**
150	−29.50	−556.34	−585.84	−29.98	−787.76	−817.74	**V8**, **D9**, **G10**, **A11**, **G12**, **K13**, **R14**, L52, F70, **R95**, Y103, **D163**, Y165, **E166**

hydrogen bonds present before simulation were retained throughout dynamics simulation. The backbone of the ligand, which was allowed to vary in the simulation, is fairly stable and the interaction involves residues Asp9, Lys13 and Arg95 being retained throughout. Thus, the designed inhibitor remains bound in the presence of the explicit solvent.

Selectivity of the designed inhibitor

The selectivity of the designed peptide inhibitor for TMPK*mt* was checked by docking it with TMPK*h* [PDB Id: 1E99]. The designed tripeptide (WPD) is involved in a network of 16 hydrogen bonds with ten residues in the case of TMPK*mt* while only nine hydrogen bonds with five residues of TMPK*h* were observed. The N-terminal of the tripeptide forms hydrogen bonds with side chain atoms of Arg97, Glu149 and Glu152 in TMPK*h* similar to that observed with the corresponding residues Arg95, Asp163 and Glue166 in TMPK*mt* (Figs. 5 and 3b). The difference in conformation of the P-loop in TMPK*mt* and TMPK*h* may contribute significantly toward the selectivity of the tripeptide for TMPK*mt*. However, the carboxy-terminal does not form any hydrogen bond in TMPK*h* due to the partially closed conformation of P-loop unlike in TMPK*mt* where the P-loop exists in the closed conformation and thus is able to form a network of seven hydrogen bonds. The carbonyl oxygen of Pro (P) forms a hydrogen bond with side chain oxygen of Ser20 and side chain nitrogen of Arg97 in TMPK*h* while it is hydrogen bonded to side chain nitrogen of Lys13 and Arg95 in TMPK*mt*. The conformation adopted by side chain atoms of Asp (P) in the two proteins was found to be different. The alteration in conformation of Asp (P) side chain can be attributed to the difference in nature of the residues present in TMPK*mt* and TMPK*h*. The side chain of Asp (P) folds back and forms two hydrogen bonds with the side chain of Arg45 in TMPK*h* while this interaction is lost due to the presence of corresponding residue Tyr39 in

Table 4 Selectivity of designed ligand (WPD)

	Target	Corresponding K_d value at 298K (nM)	Selectivity ratio
1	TMPK*mt*	0.02	1
2	TMPK*h*	426	21300

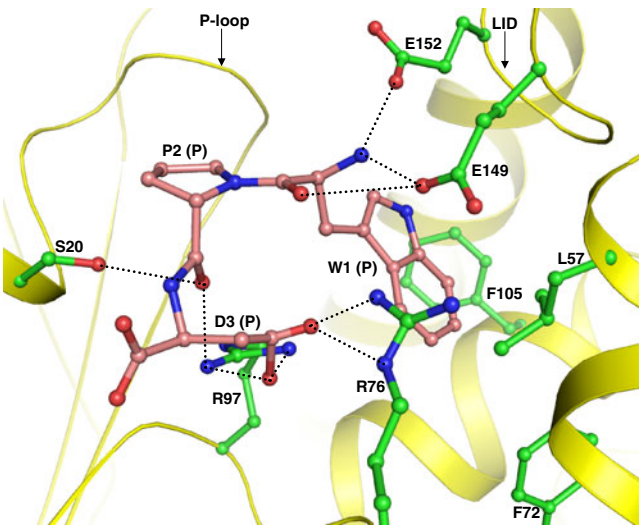

Fig. 5 Final docked position of the designed peptide inhibitor, WPD (red, ball-and-stick) with TMPK*h*

TMPK*mt* (Figs. 5 and 3b). The docking energy obtained was also higher (−167.27 kcal mol^{-1}) as compared to TMPK*mt* (−266.87 kcal mol^{-1}) (Table 2) and the predicted K_i value is 0.43 μM. Thus the modeling studies predict the tripeptide WPD to be more than 21,000-fold selective for TMPK*mt* over TMPK*h*.

The ADMET predictions indicate that the tripeptide is likely to have good oral bioavailability, absorption and permeation as identified from Lipinski's rule of five. It has molecular weight of 415 Da, a calculated logP value of 0.59, three hydrogen bond donors and seven hydrogen bond acceptors and satisfies all the criteria of Lipinski's "rule of 5" [39, 40]. Although peptides are generally known to have undesirable pharmacokinetic properties, yet they have provided novel lead compounds and, in several cases, modified peptide analogues have been developed as drugs [43]. Also, with recent advances in drug delivery techniques, the opportunities for peptide drug development have been significantly enhanced [44].

Conclusions

The overall fold of TMPK*mt* is similar to that of other known TMPKs despite the low sequence identity which ranges from 22–26%. Hence, we have exploited the sequence and structural differences between TMPK*m*t and TMPK*h* to design a potent and selective small peptide inhibitor of TMPK*mt* using an *in silico* structure-based approach. Docking studies indicate that the designed tripeptide Trp-Pro-Asp has about 25,000 times higher affinity than that of its natural substrate dTMP and it has about 33,000 higher affinity than the best reported inhibitor for TMPK*mt*. Thus the designed tripeptide, WPD, is a suitable lead compound for the development of a novel class of selective drugs for anti-tubercular therapy.

References

1. Tuberculosis (as of 17 March 2009) ->Estimated TB ->Estimated TB deaths (MDG indicator 23). WHO Global Tuberculosis Database
2. Chan ED, Iseman MD (2002) Current medical treatment for tuberculosis. Br Med J 325:1282–1286
3. Corbett EL, Watt CJ, Walker N, Maher D, Williams BG, Raviglione MC, Dye C (2003) The growing burden of tuberculosis: global trends and interactions with the HIV epidemic. Arch Intern Med 163:1009–1021
4. Nachega JB, Chaisson RE (2003) Tuberculosis drug resistance: a global threat. Clin Infect Dis 36(Suppl 1):S24–S30
5. Raviglione MC, Smith IM (2007) XDR tuberculosis - implications for global public health. N Engl J Med 356:656–659
6. Anderson EP (1973) Nucleoside and nucleotide kinases. In: Boyer PD (ed) The Enzymes; Vol 9. Academic, New York, pp 49–96
7. Sassetti CM, Boyd DH, Rubin EJ (2003) Genes required for mycobacterial growth defined by high density mutagenesis. Mol Microbiol 48:77–84
8. Pochet S, Dugué L, Douguet D, Labesse G, Munier-Lehmann H (2002) Nucleoside analogues as inhibitors of thymidylate kinases: possible therapeutic applications. Chem BioChem 3:108–110
9. Pochet S, Dugué L, Labesse G, Delepierre M, Munier-Lehmann H (2003) Comparative study of purine and pyrimidine nucleoside analogues acting on thymidylate kinases of Mycobacterium tuberculosis and of humans. Chem BioChem 4:742–747
10. Vanheusden V, Van Rompaey P, Munier-Lehmann H, Pochet S, Herdewijn P, Van Calenbergh S (2003) Thymidine and thymidine-5′-O-monophosphate analogues as inhibitors of Mycobacterium tuberculosis thymidylate kinase. Bioorg Med Chem Lett 13:3045–3048
11. Vanheusden V, Munier-Lehmann H, Froeyen M, Dugue L, Heyerick A, De Keukeleire D, Pochet S, Busson R, Herdewijn P, Van Calenbergh S (2003) 3′-C-branched-chain-substituted nucleosides and nucleotides as potent inhibitors of Mycobacterium tuberculosis thymidine monophosphate kinase. J Med Chem 46:3811–3821
12. Vanheusden V, Munier-Lehmann H, Froeyen M, Busson R, Rozenski J, Herdewijn P, Van Calenbergh S (2004) Discovery of bicyclic thymidine analogues as selective and high-affinity inhibitors of Mycobacterium tuberculosis thymidine monophosphate kinase. J Med Chem 47:6187–6194
13. Van Rompaey P, Nauwelaerts K, Vanheusden V, Rozenski J, Munier-Lehmann H, Herdewijn P, Van Calenbergh S (2003) Mycobacterium tuberculosis thymidine monophosphate kinase inhibitors: biological evaluation and conformational analysis of 2¢- and 3¢-modified thymidine analogues. Eur J Org Chem 2003:2911–2918
14. Van Daele I, Munier-Lehmann H, Hendrickx PMS, Marchal G, Chavarot P, Froeyen M, Qing L, Martins JC, Van Calenbergh S (2006) Synthesis and biological evaluation of bicyclic nucleosides as inhibitors of M. tuberculosis thymidylate kinase. ChemMedChem 1:1081–1090
15. Van Daele I, Munier-Lehmann H, Froeyen M, Balzarini J, Van Calenbergh S (2007) Rational design of 5′-thiourea-substituted α-thymidine analogues as thymidine monophosphate kinase inhibitors capable of inhibiting mycobacterial growth. J Med Chem 50:5281–5292
16. Haouz A, Vanheusden V, Munier-Lehmann H, Froeyen M, Herdewijn P, Van Calenbergh S, Delarue M (2003) Enzymatic and structural analysis of inhibitors designed against Mycobacterium tuberculosis thymidylate kinase. New insights into the phosphoryl transfer mechanism. J Biol Chem 278:4963–4971
17. Munier-Lehmann H, Pochet S, Dugue L, Dutruel O, Labesse G, Douget D (2003) Design of Mycobacterium tuberculosis Thymidine monophosphate kinase inhibitors. Nucleosides Nucleotides Nucleic Acids 22:801–804
18. Vanheusden V, Munier-Lehmann H, Pochet S, Herdewijn P, Van Calenbergh S (2002) Synthesis and evaluation of thymidine-5′-O-monophosphate analogues as inhibitors of Mycobacterium tuberculosis thymidylate kinase. Bioorg Med Chem Lett 12:2695–2698
19. Perez-Perez MJ, Priego EM, Hernandez AI, Camarasa MJ, Balzarini J, Liekens S (2005) Thymidine phosphorylase inhibitors: recent developments and potential therapeutic applications. Mini-Rev Med Chem 5:1113–1123
20. Gasse C, Douguet D, Huteau V, Marchal G, Munier-Lehmanna H, Pochet S (2008) Substituted benzyl-pyrimidines targeting thymidine monophosphate kinase of Mycobacterium tuberculosis: Synthesis and in vitro anti-mycobacterial activity. Bioorg Med Chem 16:6075–6085
21. Familiar O, Munier-Lehmann H, Negri A, Gago F, Douguet D, Rigouts L, HernndezA-I CM-J, Perez-Perez M-J (2008) Exploring Acyclic Nucleoside Analogues as Inhibitors of Mycobacterium tuberculosis Thymidylate Kinase. ChemMedChem 3:1083–1093

22. Kumar A, Chaturvedi V, Bhatnagar S, Sinha S, Siddiqi MI (2009) Knowledge based identification of potent antitubercular compounds using structure based virtual screening and structure interaction fingerprints. J Chem Inf Model 49:35–42
23. Li de la Sierra I, Munier-Lehmann H, Gilles AM, Barzu O, Delarue M (2001) X-ray structure of TMP kinase from Mycobacterium tuberculosis complexed with TMP at 1.95 Å resolution. J Mol Biol 311:87–100
24. Fioravanti E, Haouz A, Ursby T, Munier-Lehmann H, Delarue M, Bourgeois D (2003) Mycobacterium tuberculosis thymidylate kinase: structural studies of intermediates along the reaction pathway. J Mol Biol 327:1077–1092
25. Fioravanti E, Adam V, Munier-Lehmann H, Bourgeois D (2005) The crystal structure of Mycobacterium tuberculosis Thymidylate kinase in complex with 3′-azidodeoxythymidine monophosphate suggests a mechanism for competitive inhibition. Biochemistry 44:130–137
26. Ostermann N, Schlichting I, Brundiers R, Konrad M, Reinstein J, Veit T, Goody RS, Lavie A (2000) Insights into the phosphoryl transfer mechanism of human thymidylate kinase gained from crystal structures of enzyme complexes along the reaction coordinate. Structure 8:629–642
27. Ostermann N, Lavie A, Padiyar S, Brundiers R, Veit T, Reinstein J, Goody RS, Konrad M, Schlichting I (2000) Potentiating AZT activation: structures of wild-type and mutant human thymidylate kinase suggest reasons for the mutants' improved kinetics with the HIV prodrug metabolite AZTMP. J Mol Biol 304:43–53
28. Ostermann N, Segura-Pena D, Meier C, Veit T, Monnerjahn C, Konrad M, Lavie A (2003) Structures of human thymidylate kinase in complex with prodrugs: implications for the structure-based design of novel compounds. Biochemistry 42:2568–2577
29. Discovery Studio 1.7 (2006) molecular modeling program package. Accelrys Software Inc, San Diego
30. Berman HM, Westbrook J, Feng Z, Gilliland G, Bhat TN, Weissig H, Shindyalov IN, Bourne PE (2000) The protein data bank. Nucleic Acids Res 28:235–242
31. Brooks BR, Bruccoleri RE, Olafson BD, States DJ, Swaminathan S, Karplus M (1983) CHARMM: a program for macromolecular energy, minimization, and dynamics calculations. J Comput Chem 4:187–217
32. Momany FA, Rone R (1992) Validation of the general purpose QUANTA ®3.2/CHARMm® force field. J Comput Chem 13:888–900
33. Venkatachalam CM, Jiang X, Oldfield T, Waldman M (2003) LigandFit: a novel method for the shape-directed rapid docking of ligands to protein active sites. J Mol Graphics Modell 21:289–307
34. Mayo SL, Olafson BD, Goddard WA III (1990) Dreiding: a generic force forcefield for molecular simulation. J Phys Chem 94:8897–8909
35. Böhm HJ (1994) The development of a simple empirical scoring function to estimate the binding constant for a protein-ligand complex of known three-dimensional structure. J Comput Aided Mol Des 8:243–256
36. Böhm HJ (1994) On the use of LUDI to search the fine chemicals directory for ligands of proteins of known three-dimensional structure. J Comput Aided Mol Des 8:623–632
37. Böhm HJ (1998) Prediction of binding constants of protein ligands: a fast method for the prioritization of hits obtained from de novo design or 3D database search programs. J Comput Aided Mol Des 12:309–323
38. Wang R, Lu Y, Wang S (2003) Comparative evaluation of 11 scoring functions for molecular docking. J Med Chem 46:2287–2303
39. Lipinski CA (2001) Drug-like properties and the causes of poor solubility and poor permeability. J Pharmacol Toxicol Methods 44:235–249
40. Lipinski CA, Lombardo F, Dominy BW, Feeney JP (2001) Experimental and computational approaches to estimate solubility and permeability in drug discovery and development setting. Adv Drug Deliv Rev 46:3–26
41. Berendsen HJC, Postma JPM, DiNola A, van Gunsteren WF, DiNola A, Haak JR (1984) Molecular dynamics with coupling to an external bath. J Chem Phys 81:3684–3690
42. Munier-Lehmann H, Chaffotte A, Pochet S, Labesse G (2001) Thymidylate kinase of Mycobacterium tuberculosis: a chimera sharing properties common to eukaryotic and bacterial enzymes. Protein Sci 10:1195–1205
43. Ayoub M, Scheidegger T (2006) Peptide drugs, overcoming the challenges, growing business. Chem Today 24:46–48
44. Otvos L (2008) Peptide-based drug design: here and now. In: Clifton NJ (ed) Methods mol biol Series, vol-494, pp 1-8
45. DeLano WL (2002) The PyMOL Molecular Graphics System on World Wide Web http://www.pymol.org